Available online at www.sciencedirect.com
SCIENCE DIRECT®
Thermochimica Acta 142 (2004) 97–105
thermochimica acta
www.elsevier.com/locate/tca

Synthesis, characterization, and thermal decomposition of oxamido heterobinuclear Cu(II)–Ln(III) complexes

Hai-Dong Wang [a,b], Yong Chen [c], Yan-Tuan Li [a], Xian-Cheng Zeng [a,*]

[a] *Faculty of Chemistry, Sichuan Key Laboratory of Green Chemistry and Technology, Sichuan University, Chengdu 610064, PR China*
[b] *Qinghai Institute of Salt Lakes, The Chinese Academy of Sciences, Xining 810008, PR China*
[c] *Department of Applied Oil Engineering, Logistical Engineering University, Chongqing 400016, PR China*

Received 11 October 2002; received in revised form 2 September 2003; accepted 8 September 2003

Abstract

Three oxamido-bridged copper(II)–lanthanide(III) heterobinuclear complexes described by the overall formula Cu(oxen)Ln(phen)$_2$(ClO$_4$)$_3$ (oxen = *N*,*N*′-bis(2-aminoethyl)oxamide, Ln = Eu, Gd, and Er, phen = 1,10-phenanthroline), have been synthesized and characterized by the elemental analyses, IR spectroscopy, X-ray analysis and energy dispersive spectrometer (EDS) analysis. The thermal decomposition of the complexes was studied by TG, DTG, and DTA technique under dynamic nitrogen atmosphere. The decompositions of these complexes took place through four stages. The second and third stages were analyzed kinetically by means of the Achar method and the Coats–Redfern method. The activation energies, pre-exponential factors and the most probable kinetic model function were determined for these stages.

Keywords: Cu(II)–Ln(III) heterobinuclear complex; Thermal decomposition; Non-isothermal kinetic

1. Introduction

The interest in bridged heteroplymetallic systems with two different paramagnetic centers has risen considerable in recent years [1]. The synthesis, spectroscopic and magnetic investigations of new heterobinuclear complexes are important not only for gaining some insight into the electronic and geometric structure of metalloproteins and enzymes and thus the correlating structure with biological function, but also for obtaining information about designing and synthesizing molecule-based magnets and investigating the spin-exchange mechanism between paramagnetic metal ions. But to this end, few studies on thermochemistry, so far as we know, have been reported.

As part of our continuous work, the coordination environment of the title complexes had been measured by different analysis technique. The results indicate that their coordination environment is very similar to that of the single crystal [Cu(oxap)Ni(phen)$_2$](ClO$_4$)$_2$·2H$_2$O [2]. In this paper, we study the thermal decompositions of the complexes of Cu(oxen)Ln(phen)$_2$(ClO$_4$)$_3$ (Ln = Eu, Gd and Er) by means of thermal analyses.

Corresponding to Scheme 1, the coordination environment of oxamido heterobinuclear Cu(II)–Ln(III) complex was drawn below.

2. Experiment

2.1. Materials

All materials were commercial products of chemical or analytic grade purity and were used without further purification. The mononuclear complex as "ligands" of *N*,*N*′-bis(2-aminoethyl)oxamidocopper(II) complex was prepared by previously published procedures [3]. Three compounds of the hydrated lanthanide(III) perchlorate was prepared by general methods.

2.2. Synthesis of binuclear Cu(II)–Gd(III) complexes

The methods used to prepare three copper(II)–lanthanide-(III) heterobinuclear complexes were virtually identical and were exemplified by Cu(oxen)Eu(phen)$_2$(ClO$_4$)$_3$·2H$_2$O. A solution of Cu(oxen) (0.265 g, 1 mmol) in absolute

* Corresponding author.
E-mail address: zengxc@pridns.scu.edu.cn (X.-C. Zeng).

0040-6031/$ – see front matter © 2003 Elsevier B.V. All rights reserved.
doi:10.1016/j.tca.2003.09.006

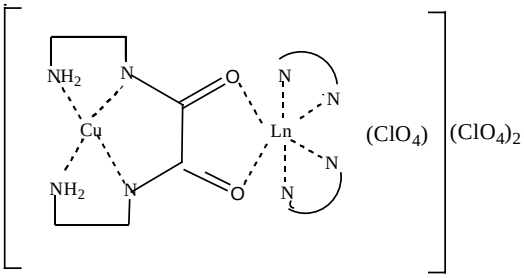

Scheme 1. The coordination environment of oxamido heterobinuclear Cu(II)–Ln(III) complex.

ethanol (15 cm^3) was added successively a solution of $Eu(ClO_4)_3{\cdot}6H_2O$ (0.56 g, 1 mmol) in absolute ethanol (15 cm^3) with stirring at room temperature. Then the mixed solution was added an absolute ethanol solution (25 cm^3) of 1,10-phenanthroline (0.4 g, 2 mmol). The color of the solution turned from violet-red to Cambridge blue immediately and a small amount of precipitate formed. After stirring for ca. 12 h, the resultant Cambridge blue microcrystals were filtered off, washed several times with absolute ethanol and diethyl ether and dried under reduced pressure.

All analytical data and colors of the binuclear complexes are collected in Table 1.

2.3. Physical measurements

Carbon, hydrogen and nitrogen elemental analyses were performed with a Perkin-Elmer elemental analyzer Model 240. Metal contents were determined by EDTA titration. IR spectra were recorded with a Nicolet FT-IR spectrophotometer using KBr pellets. Molar conductances were measured with a DDS-11A conductometer. TG–DTG–DTA was carried out on a TGDTA92 simultaneous analyzer (Setaram Corp.). TG–DTA runs were carried out at a heating rate of 10 °C min^{-1} under a dynamic nitrogen atmosphere using a flow rate of 40 cm^3 min^{-1}, and the temperature range was 20–1300 °C. The reference was α-Al_2O_3. Alumina crucibles were used to hold 2–3 mg samples for analyses. The X-ray analysis is carried out by means of a Riemens D/Max III B powder diffractometer, using Cu Kα radiation. EDS analysis is carried out by means of KEVEX-Sigma energy dispersive spectrometer.

3. Results and discussions

3.1. General properties of the binuclear complexes

These binuclear complexes are very soluble in acetonitrile, DMF and DMSO to give stable solutions at room temperature; moderately soluble in water, methanol and acetone, and practically insoluble in carbon tetrachloride, chloroform and benzene. The $Cu(oxen)Ln(phen)_2(ClO_4)_3$ (Ln = Eu, Gd, and Er) complex can be recrystallized from a DMF/ethanol (1:2) mixture. In the solid state all of the Cu(II)–Ln(III) binuclear complexes are fairly stable in air, thus allowing physical measurements. For the three Cu(II)–Ln(III) binuclear complexes, the observed molar conductance values in DMF solution due to 1:2 ionic complexes. These values indicated that only one ClO_4^- anion exist in the inner-spheres of these complexes. This is consistent with the measured IR data of the heterobinuclear complexes.

3.2. Infrared spectra

Since the IR spectra of the three binuclear complexes are similar, the discussion is confined to the most important vibrations of the 200–4000 cm^{-1} region in relation to the structure. The IR absorption bands of the complexes are given in Table 2. We will only discuss the selected infrared bands, with most relevant IR absorption bands from the IR spectra of the binuclear complexes and the mononuclear fragment *N*,*N*′-bis(2-aminoethyl)oxamidocopper(II). The carbonyl stretching vibration at 1585 cm^{-1} for the mononuclear fragment Cu(oxen)is considerably shifted towards higher frequencies (ca. 60–70 cm^{-1}) in the binuclear complexes. Therefore, in general, when the deprotonated amide nitrogen is coordinated to the metal ion, its amide band shifts considerably towards lower wavenumbers. In the case of an oxamide dianion coordinated to two metal ions as a bridging ligands, the amide band reverts to near its original position (in the protonated species) [4]. Although the amide is due to a composite N–C=O vibration, it can essentially be seen as ν(C=O). It is likely that the bond order of C=O (carbonyl) in the binuclear complexes is higher than that in the corresponding mononuclear complex Cu(oxen). This shift has often been used as a diagnostic

Table 1
Elemental analyses and colors of the binuclear complexes

Complex	Empirical formula (formula weight)	Color	Elemental analyses (calculated) (%)				
			C	H	N	Cu	Ln
(**1**)[a]	$CuEuC_{30}H_{32}N_8O_{16}Cl_3$ (1082.50)	Light-blue	33.12 (33.29)	2.70 (2.98)	10.29 (10.35)	5.90 (5.87)	14.21 (14.04)
(**2**)[b]	$CuGdC_{30}H_{32}N_8O_{16}Cl_3$ (1087.79)	Light-blue	33.17 (33.13)	2.78 (2.97)	10.20 (10.30)	5.87 (5.84)	14.40 (14.46)
(**3**)[c]	$CuErC_{30}H_{32}N_8O_{16}Cl_3$ (1097.80)	Light-blue	33.02 (32.82)	2.79 (2.94)	10.18 (10.21)	5.80 (5.79)	15.30 (15.24)

[a] $Cu(oxen)Eu(phen)_2(ClO_4)_3{\cdot}2H_2O$.
[b] $Cu(oxen)Gd(phen)_2(ClO_4)_3{\cdot}2H_2O$.
[c] $Cu(oxen)Er(phen)_2(ClO_4)_3{\cdot}2H_2O$.

Table 2
IR spectra of analytical data of the complexes

Complexes	IR (cm^{-1})				
	ν(C=O)	$\nu(NH_2)$	$\nu(ClO_4^-)$	ν(N=C)	ν(Ln–N)
$Cu(oxen)Eu(phen)_2(ClO_4)_3{\cdot}2H_2O$	1645	3250	11301020	1550	395
$Cu(oxen)Gd(phen)_2(ClO_4)_3{\cdot}2H_2O$	1650	3250	11301020	1530	380
$Cu(oxen)Er(phen)_2(ClO_4)_3{\cdot}2H_2O$	1655	3250	11301020	1530	382

indicator for oxamido-bridged structures [4]. On the other hand, the C=O deformation vibration at 720 cm^{-1} of the ligand complex, *N*,*N*′-bis(2-aminoethyl)oxamidocopper(II), disappeared in the spectra of the binuclear complexes. This fact may be attributed to the coordination of the carbonyl oxygens to the Ln(III) ion [5–7]. This coordination mode of the complex ligand, Cu(oxen), has been revealed by X-ray diffraction analysis of an analogous complex [5]. In addition, the –N=C– stretching vibration for the terminal ligand (phen) was shifted to higher frequencies (1530 cm^{-1}) in these binuclear complexes, suggesting that the N atoms of the terminal ligand coordinated with the Ln(III) ion. The additional band observed at around 380–390 cm^{-1} due to ν(Ln–N) further supports this view. However, in general, the difference in wavenumbers between the two highest frequency (1130 and 1020 cm^{-1}), indicating that the coordinated perchlorate ions is a single dentate [8]. Thus, the above spectral observations, together with the molar conductance data, confirm that the perchlorate ion is coordinated to the Ln(III) ions in a single dentate fashion in these binuclear complexes.

3.3. Energy dispersive spectrometer

The composition of three binuclear complexes were defined by energy dispersive spectrometer (EDS) analysis (shown in Figs. 1–3), respectively. The analysis results indicate that each complex contains two kinds of different metal ions. So, from these conclusions can be proved these complexes are that heterobinuclear complex.

3.4. Thermal analysis

3.4.1. $Cu(oxen)Eu(phen)_2(ClO_4)_3{\cdot}2H_2O$

The TG, DTG, and DTA curves of the $Cu(oxdn)Eu(phen)_2(ClO_4)_3{\cdot}2H_2O$ complex are shown in Fig. 4. Four stages of the dissociation of complex are indicated in TG and DTG curve. The decomposition starts from 31 °C and ends at 173 °C, the mass loss observed is 3.31% against calculated 3.33%, corresponding to the release of 2 mol of water. The second stage is from 173 to 281 °C. The mass loss observed is 8.91% against calculated 9.19%, showing that 1 mol perchlorate ion is expelled. The third stage is in continuation with the second stage from 281 to 412 °C. The mass loss

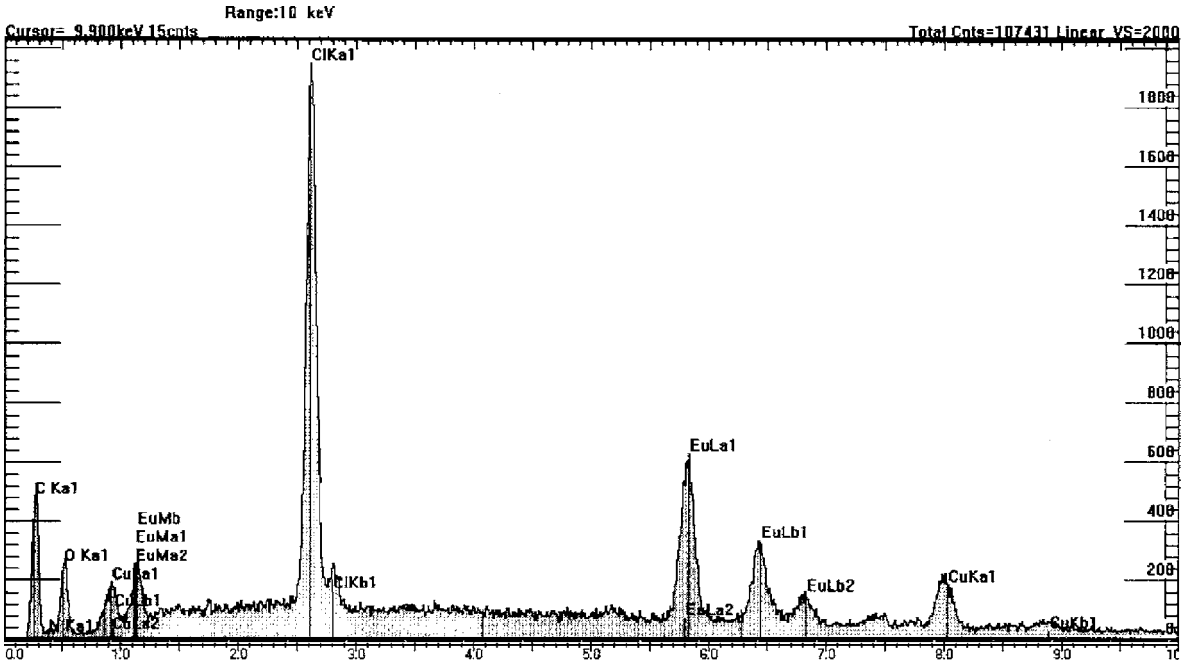

Fig. 1. Energy dispersive spectrometer of Cu(II)–Eu(III) complex.

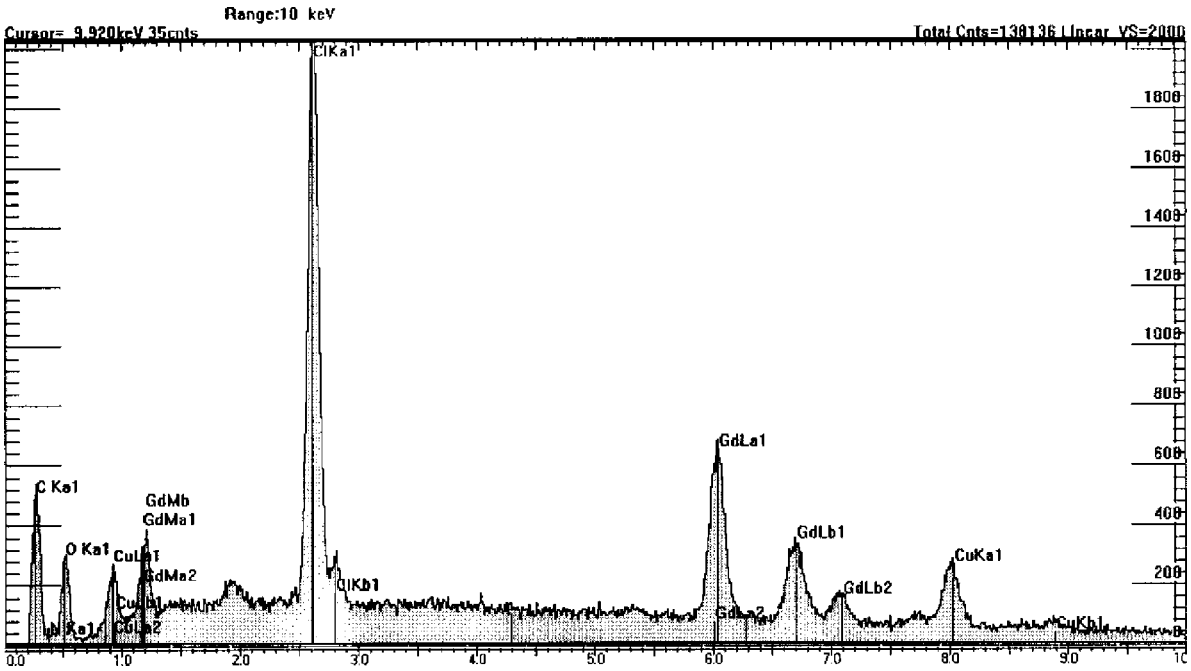

Fig. 2. Energy dispersive spectrometer of Cu(II)–Gd(III) complex.

observed is 18.36% against calculated loss of 18.37%, corresponding to the dissociation of 2 mol of perchlorate ions. The fourth stage is from 412 to 1273 °C. The mass loss observed is 39.81%, showing that organic groups are expelled. We can make out from the TG curve, trend that the mass loss descends to being slow. The results indicate that the serious product charcoal appearance has occurred the decomposition process of chemical compound. The mass loss is measured cannot to be compared with theory value. The sinters of thermal decomposition were analyzed by the X-ray powder diffraction method (shown in Fig. 5). The results shown that the final product is considered to be Eu_2O_3, Cu, and C. The thermoanalytical data for $Cu(oxen)Eu(phen)_2(ClO_4)_3{\cdot}2H_2O$ complex are listed in Table 3.

There is one weakness endothermic peak and two exothermic peaks in DTA curve corresponding to the chemical events observed in the TG curve. Especially, there is the strong peak (exothermic peak) in DTA curve, shown that

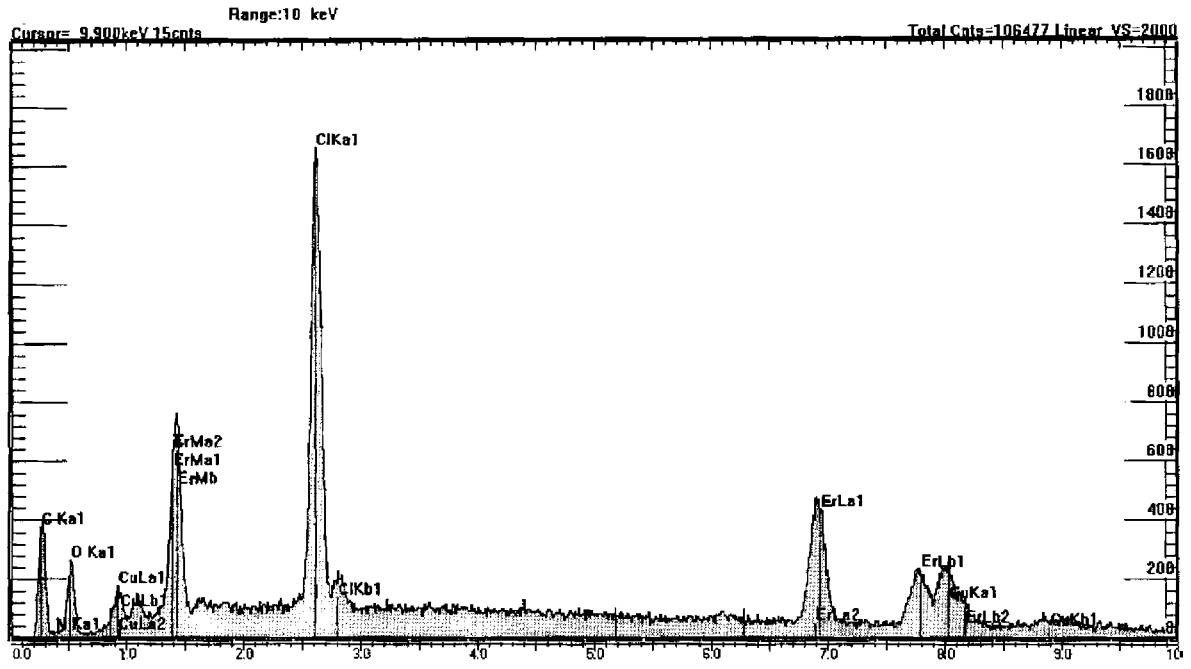

Fig. 3. Energy dispersive spectrometer of Cu(II)–Er(III) complex.

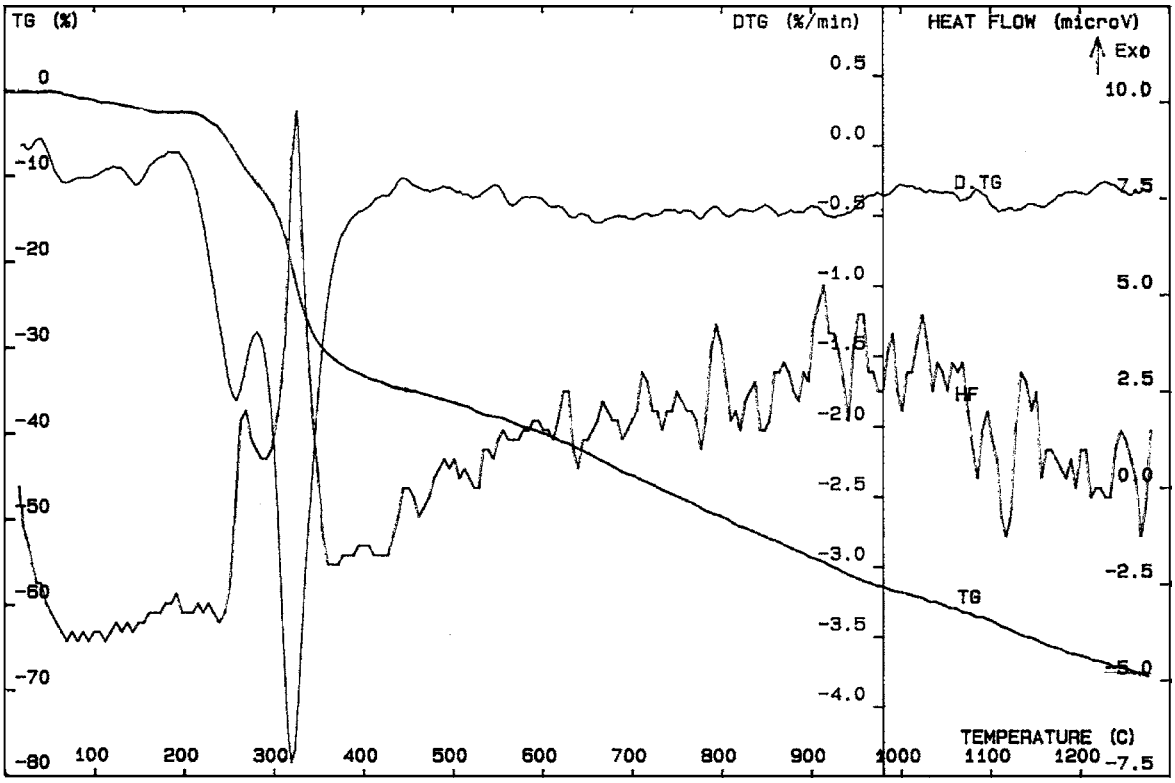

Fig. 4. TG–DTG–DTA curves of Cu(II)–Eu(III) complex.

the explosive reaction of the perchlorate ion occurs in the thermal decomposition process. Owing to the complexity of thermal decomposition reaction, we can clearly from the curve on make out that it is not smooth. All of the peak temperatures are listed in Table 3.

The thermal decomposition of different stages is shown as follows:

$$CuEuC_{30}H_{32}N_8O_{16}Cl_3 \xrightarrow{2H_2O} CuEuC_{30}H_{28}N_8O_{14}Cl_3 \xrightarrow{ClO_4^-} CuEuC_{30}H_{28}N_8O_{10}Cl_2$$

$$\xrightarrow{2ClO_4^-} CuEuC_{30}H_{28}N_8O_2 \xrightarrow{\text{organic}} Eu_2O_3+Cu+C$$

3.4.2. *Cu(oxen)Gd(phen)$_2$(ClO$_4$)$_3$·2H$_2$O*

The TG, DTG and DTA curves of Cu(oxen)Gd(phen)$_2$(ClO$_4$)$_3$·2H$_2$O complex are shown in Fig. 6. The TG and DTG curves indicate the dissociation of complex in four stages. The first transition changes from 31 to 189 °C, and the mass loss observed is 3.24% against the calculated loss

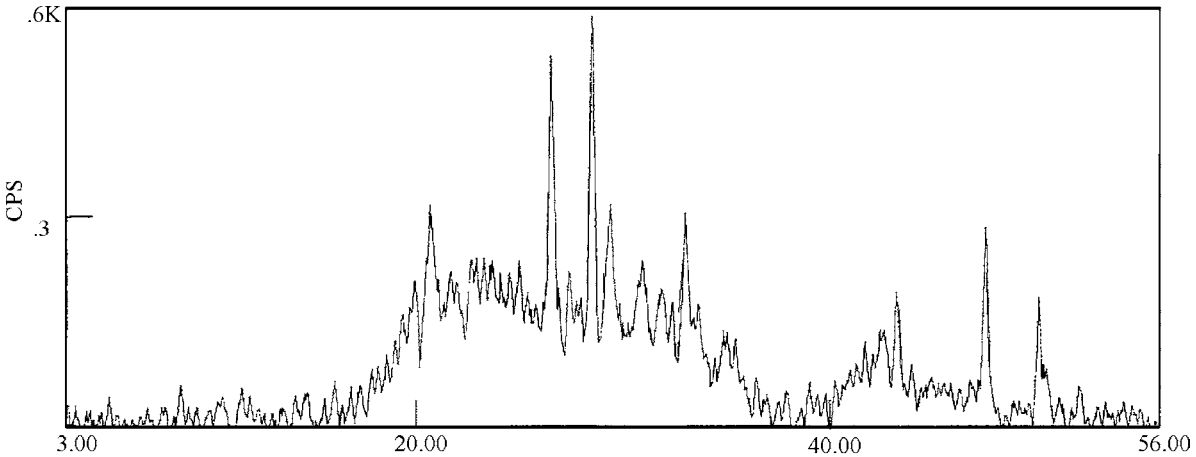

Fig. 5. Presents powder diffraction of the sinters of Cu(II)–Eu(III) complex.

Table 3
Thermal decomposition data for Cu(II)–Ln(III) complexes from TG–DTA[a]

Complexes	Stages	Decomposition temperature range (°C)	DTA, T_p (°C)	Mass loss (%)		Probably expelled composition
				TG	Theory	
Cu(II)–Eu(III)	(1)	31–173	81(endo)	3.31	3.33	$2H_2O$
	(2)	173–281	270(exo)	8.91	9.19	ClO_4^-
	(3)	281–412	324(exo)	18.36	18.37	$2ClO_4^-$
	(4)	412–1273	–	39.81	–	Organic groups
Cu(II)–Gd(III)	(1)	31–189	80(endo)	3.24	3.31	$2H_2O$
	(2)	189–282	271(exo)	8.98	9.14	ClO_4^-
	(3)	282–412	324(exo)	18.40	18.28	$2ClO_4^-$
	(4)	412–1266	–	37.89	–	Organic groups
Cu(II)–Er(III)	(1)	31–190	81(endo)	3.14	3.28	$2H_2O$
	(2)	190–285	276(exo)	8.89	9.06	ClO_4^-
	(3)	285–411	328(exo)	18.20	18.12	$2ClO_4^-$
	(4)	411–1269	–	33.64	–	Organic groups

[a] T_p: temperature of peak; endo: endothermic; exo: exothermic.

of 3.31%, corresponding to the release of 2 mol of water. The second transition is from 189 to 282 °C, and the mass loss observed is 8.98% against the calculated loss of 9.14%, due to the release of 1 mol of perchlorate ion. The third stage is in continuation with the second stage from 282 to 412 °C. The mass loss observed is 18.40% against calculated loss of 18.28%, corresponding to the dissociation of 2 mol of perchlorate ions. The fourth stage is from 412 to 1266 °C. The mass loss observed is 37.89%, showing that organic groups are expelled. The experiment result is similar to the decomposition of the first complex. We infer that this is also equally creating owing to the serious product charcoal factor. The results of X-ray powder diffraction analysis are similar with above complex. The final product is considered to be Gd_2O_3, Cu and C. The thermoanalytical data for $Cu(oxen)Gd(phen)_2(ClO_4)_3{\cdot}2H_2O$ complex are also given in Table 3.

All transitions in DTA curve corresponding to the transition observed in the TG curve. The shape of DTA curve is similar to the first complex. The result explains that thermal

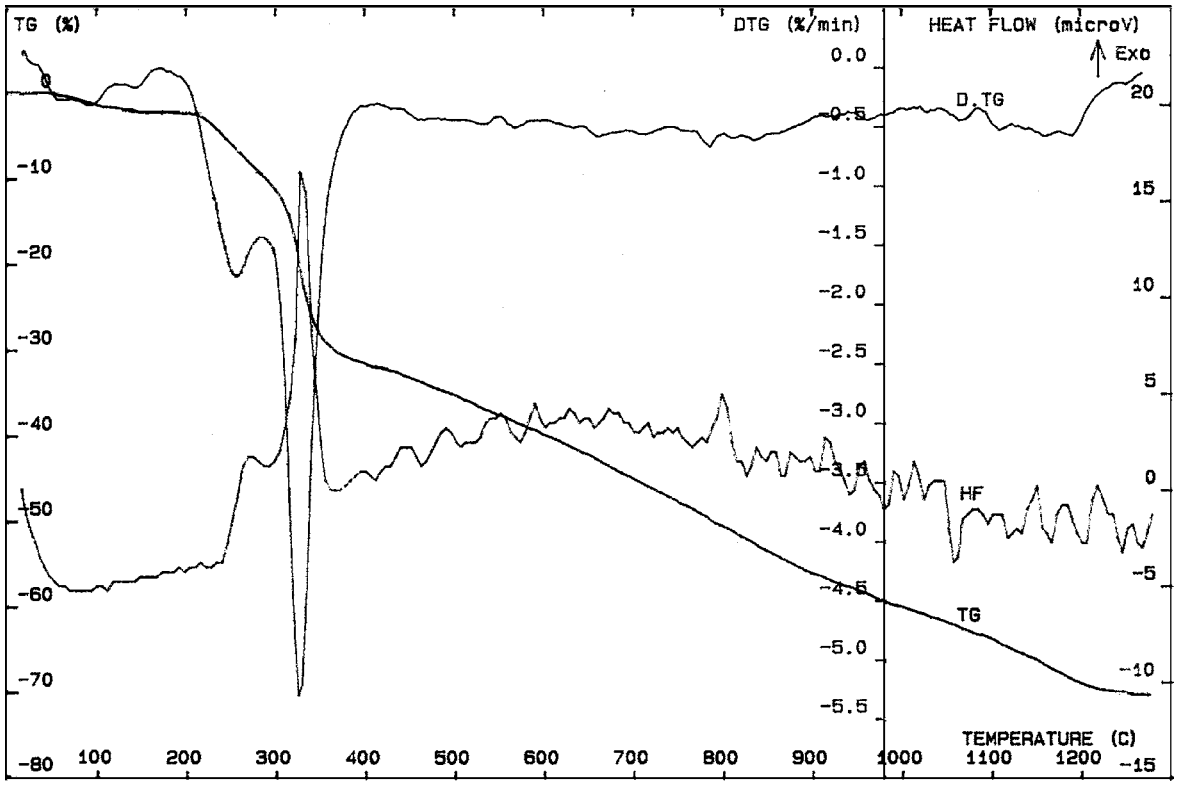

Fig. 6. TG–DTG–DTA curves of Cu(II)–Gd(III) complex.

decomposition processes of the second complex are each other similar with the first complex. All of the peak temperatures are also given in Table 3.

The sequential thermal dissociation process of the complex is shown as follows:

$$CuGdC_{30}H_{32}N_8O_{16}Cl_3 \xrightarrow{2H_2O} CuGdC_{30}H_{28}N_8O_{14}Cl_3 \xrightarrow{ClO_4^-} CuGdC_{30}H_{28}N_8O_{10}Cl_2$$

$$\xrightarrow{2ClO_4^-} CuGdC_{30}H_{28}N_8O_2 \xrightarrow{organic} Gd_2O_3+Cu+C$$

3.4.3. *Cu(oxen)Er(phen)$_2$(ClO$_4$)$_3$·2H$_2$O*

The TG, DTG and DTA curves of Cu(oxen)Er(phen)$_2$(ClO$_4$)$_3$·2H$_2$O complex are shown in Fig. 7. Four stages the transitions observed in the TG curve and DTG curves. The first transition changes from 31 to 191 °C, and the mass loss observed is 3.14% against the calculated loss of 3.28%, corresponding to the release of 2 mol of water. The second transition is from 191 to 285 °C, and the mass loss observed is 8.89% against the calculated loss of 9.06%, due to the release of 1 mol of perchlorate ion. The third stage is in continuation with the second stage from 285 to 411 °C. The mass loss observed is 18.20% against calculated loss of 18.12%, corresponding to the dissociation of 2 mol of perchlorate ions. The fourth stage is from 411 to 1269 °C. The mass loss observed is 33.64%, showing that organic groups are expelled. The experiment result is similar to the decomposition of the above two complexes, and X-ray powder diffraction analysis are similar with above two complexes. The final product is considered to be Er$_2$O$_3$, Cu and C. The thermoanalytical data for Cu(oxen)Er(phen)$_2$(ClO$_4$)$_3$·2H$_2$O complex are also given in Table 3.

All transitions in DTA curve corresponding to the transition observed in the TG curve. The shape of DTA curve is similar to the above two complexes. The result explains that thermal decomposition processes of the two complexes are each other similar with the first complex. All of the peak temperatures are also given in Table 3.

The sequential thermal dissociation process of the complex is shown as follows:

$$CuErC_{30}H_{32}N_8O_{16}Cl_3 \xrightarrow{2H_2O} CuErC_{30}H_{28}N_8O_{14}Cl_3 \xrightarrow{ClO_4^-} CuErC_{30}H_{28}N_8O_{10}Cl_2$$

$$\xrightarrow{2ClO_4^-} CuErC_{30}H_{28}N_8O_2 \xrightarrow{organic} Er_2O_3+Cu+C$$

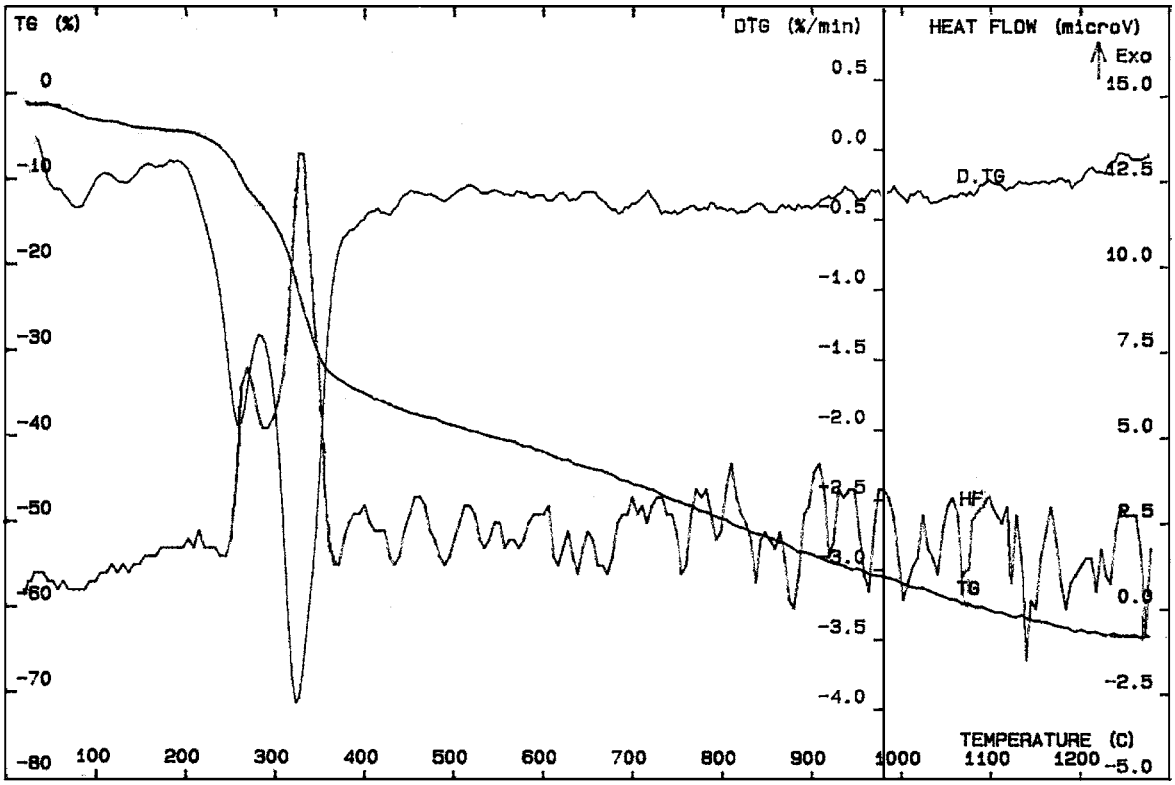

Fig. 7. TG–DTG–DTA curves of Cu(II)–Er(III) complex.

Table 4
The stage's kinetic model function of Cu(II)–Ln(III) complex

Metal complex	Stage	Function no.	Integral method			Differential method		
			E (kJ mol^{-1})	ln A (s^{-1})	r	E (kJ mol^{-1})	ln A (s^{-1})	r
Cu(II)–Eu(III)	(2)	4	231.63	53.84	0.9901	242.12	53.62	0.9924
	(3)	18	201.21	43.44	0.9762	215.32	40.90	0.9861
Cu(II)–Gd(III)	(2)	4	248.50	56.06	0.9898	263.72	53.86	0.9886
	(3)	18	223.11	47.75	0.9918	248.34	47.44	0.9908
Cu(II)–Er(III)	(2)	4	260.36	59.84	0.9890	272.01	55.40	0.9870
	(3)	18	254.38	53.89	0.9814	272.46	52.24	0.9864

From the view of coordination chemistry, each of the similar decomposition steps of three complexes has the same origin. The material losses for every decomposition step are conjectured based on the percentages of weight losses. Comparing with the temperature of decomposition of three complexes, their relative thermal stability can be obtained as follow: Cu(oxen)Eu(phen)$_2$(ClO$_4$)$_3$·2H$_2$O < Cu(oxen)Gd(phen)$_2$(ClO$_4$)$_3$·2H$_2$O < Cu(oxen)Er(phen)$_2$(ClO$_4$)$_3$·2H$_2$O. In addition, the results of the final produce for three complexes indicted that the between different metal ion interaction is exist in coordination environment, because the lanthanide ion changed oxide with heating, and copper ion reduced. Unfortunately, as an incline (no clear plateau) appears on the TG curve in fourth step, it cannot concluded obviously thermal transition, and cannot explain clearly thermochemical manifestation of the between different metal ion interaction.

3.5. Kinetic studies of non-isothermal decomposition

This analysis was carried out for second stage of the thermal decomposition process of each complex.

In this paper, the Achar et al. [9] and the Coats–Redfern [10] methods were employed to derive the kinetic parameter and a possible kinetic model function of thermal decomposition was suggested by comparing the kinetic parameters.

The integral and differential equations are as follows:

$$\ln\left[\frac{\mathrm{d}\alpha/\mathrm{d}t}{f(\alpha)}\right] = \ln A - \frac{E}{RT} \quad (1)$$

$$\ln\left[\frac{g(\alpha)}{T^2}\right] = \ln\left(\frac{AR}{\beta E}\right) - \frac{E}{RT} \quad (2)$$

where α is the fraction of decomposition, T the absolute temperature, β the heating rate, E the activation energy in kJ mol^{-1}, A the pre-exponential factor, R the gas constant in kJ mol^{-1} K^{-1}, $f(\alpha)$ and $g(\alpha)$ are the kinetic model functions [11].

The basic parameters of second and third stages of T, α, and dα/dt obtained from the TG and DTG curves of Cu(oxen)Eu(phen)$_2$(ClO$_4$)$_3$·2H$_2$O, Cu(oxen)Gd(phen)$_2$(ClO$_4$)$_3$·2H$_2$O, and Cu(oxen)Er(phen)$_2$(ClO$_4$)$_3$·2H$_2$O complexes. The kinetic analysis was completed with the linear least-squares method. Comparing the kinetic parameters from different methods, we selected the probable kinetic model function by which the calculated values of E and ln$A$ were close to each other with the better linear correlation coefficient. Then, it can be concluded that kinetic equation of thermal decomposition of the complexes for the second and third stage. The calculated values of the kinetic parameters of complex for obvious transition and the probable kinetic model functions are listed in Table 4.

The results of second stage indicate that the two E values are approximately equal, so also are the two ln$A$ values, and the linear correlation coefficients are best when the function number 4 [11] was taken as the most probable mechanism function for Cu(oxen)Eu(phen)$_2$(ClO$_4$)$_3$·2H$_2$O. The same parameters were given for Cu(oxen)Gd(phen)$_2$(ClO$_4$)$_3$·2H$_2$O and Cu(oxen)Er(phen)$_2$(ClO$_4$)$_3$·2H$_2$O. Their mechanism functions were also number 4. The mechanism functions of the thermal decomposition of three complexes for the third stage were number 18 [11].

Where, the mechanism function number 4 is Jander equation, $g(\alpha) = [1-(1-\alpha)^{1/3}]^2$ and $f(\alpha) = (3/2)(1-\alpha)^{2/3}[1-(1-\alpha)^{1/3}]^{-1}$, which belongs to a three-dimensional diffusion (spherical symmetry). The mechanism function number 18 is second order equation, $g(\alpha) = (1-\alpha)^{-1} - 1$ and $f(\alpha) = (1-\alpha)^2$, which belongs to chemical reaction.

According to the above results, three complexes have the same structure and the same coordination environment, because the calculated values of the activation energy and the pre-exponential factor were close to second and third step of the thermal decomposition. But the kinetic analysis of the final step decomposition was not studied due to the serious product charcoal appearance has occurred the decomposition process of chemical compound. Otherwise, the relative thermal stability of three complexes can be obtained again from the values of E for second and third step decomposition.

Acknowledgements

This work has been supported by the National Natural Science Foundation of China (Grant No. 20173038).

References

[1] R.D. Willett, D. Gatteschi, O. Kahn (Eds.), Magneto-Structural Correlation in Exchange Coupled Systems, Reidel, Dordrecht, 1985, pp. 523–554.
[2] D.Z. Liao, L.C. Li, Z.H. Jiang, S.P. Yan, P. Cheng, G.L. Wang, Trans. Met. Chem. 17 (1992) 250.
[3] Y. Journaux, J. Sletten, O. Kahn, Inorg. Chem. 24 (1985) 4063.
[4] H. Ojima, K. Nonoyama, Coord. Chem. Rev. 92 (1988) 85.
[5] Y.-T. Li, D.Z. Liao, Z.H. Jiang, G.L. Wang, Polyhedron 14 (1995) 2209.
[6] Y.-T. Li, Z.H. Jiang, S.L. Ma, D.Z. Liao, S.P. Yan, G.L. Wang, Polyhedron 23 (1993) 2781.
[7] E. Lioret, Y. Journaux, M. Julve, Inorg. Chem. 29 (1990) 3967.
[8] Y.-T. Li, M.M. Miao, D.Z. Liao, Z.H. Jiang, G.L. Wang, Polish J. Chem. 69 (1995) 1402.
[9] B.N. Achar, G.W. Brindley, J.H. Sharp, Proceedings of the International Clay Conference, Jerusalem, vol. 1, 1966.
[10] A.W. Coats, J.P. Redfern, Nature 201 (1964) 68.
[11] X. Gao, D. Dollimore, Thermochim. Acta 47 (1993) 215.